2D versus 1D ground-motion modelling for the Friuli region, north-1 eastern Italy

W. Imperatori, Hideo Aochi, P. Suhadolc, John Douglas, Ariane Ducellier, G. Costa

2D versus 1D ground-motion modelling for the Friuli region, north-eastern Italy

W. Imperatori[1, *], H. Aochi[2, †], P. Suhadolc[1], J. Douglas[2], A. Ducellier[2], G. Costa[1]

[1] Dipartimento di Scienze della Terra, Università degli Studi di Trieste, via E. Weiss 1, 34127 Trieste, Italy.

[2] Natural Risks and CO2 Storage Security Division, BRGM, 3 avenue C. Guillemin, 45060 Orléans Cedex 2, France.

Abstract

We perform a series of simulations of seismic wave propagation from potential earthquakes to evaluate how the 2D (in the NW-SE direction) geological structure of the Friuli (NE Italy) basin affects ground motions, particularly in terms of peak ground velocity (PGV). The decay of PGV with source-receiver distance from the 2D modelling is compared to that obtained from 1D modelling, using a standard model for seismological studies in this region, one obtained by averaging the 2D model along the source-receiver distance and one based on the local structure under the receiver. Synthetic seismograms are computed using a finite-difference technique for point sources with an upper frequency cut-off of 0.6 Hz. 2D effects are clearly seen, particularly in the centre of the sedimentary basin, for certain earthquake scenarios. The analysis of the role played by the main heterogeneities on the propagating wavefield permits us to conclude that an acceptable fit to the 2D PGV values for the entire section is possible using a series of 1D models for the Friuli region except for shallow earthquakes located to the north-west of the basin, where the structure of the basin edge is complex.

[*] **Current address: Institute of Geophysics, ETH Zurich, HPP G.1.1, Schafmattstrasse 30, CH-8093 Zurich, Switzerland.**

[†] **Corresponding author: h.aochi@brgm.fr**

Introduction

In well-studied regions, such as California, 3D geological structure models are often used for ground-motion modelling, since they show significant differences to predictions based on 1D structures (e.g. Graves and Wald, 2001; Wald and Graves, 2001; Liu and Archuleta, 2004). However, information on the 2D or 3D velocity crustal structure of many regions of the world is still largely unavailable. Even in areas where such information has been published, 1D models are still preferred for many seismological applications. In some analyses, different 1D models are chosen for different stations to better characterize the structure between source and certain receivers, as seen in Wu et al. (2001) for the Chi-Chi earthquake and Liu et al. (2006) for the 2004 Parkfield earthquake, for example. This is because both analytical and semi-analytical methods (e.g. modal summation and reflectivity methods), which are widely used to produce synthetic seismograms for forward modelling and inverse analysis, are often formulated for a 1D, vertically heterogeneous but horizontally uniform, model. Although such 1D approximation is not better than any well-calibrated 2D or 3D model, numerous studies [e.g. those of Wu et al. (2001) and Liu et al. (2006)] imply that a station-adjusted 1D model can provide reasonably accurate ground motion predictions. In this article, we ask these related questions for the Friuli region, north-eastern Italy, (see Figure 1) not for the analysis of the earthquake source but for the purpose of ground motion prediction. How important is the 2D basin effect in the Friuli region? How well are 1D models able to reproduce the main features of ground motion simulated using 2D models?

A new, laterally-heterogeneous 2D model based on a geological section cutting from the NW to the SE of Friuli is proposed in Figure 2(a). As can be seen, this model displays quite complex geological features in the NW, due to thrust activities in that part of the region, while the middle and the SE sections are noticeably simpler. In several previous papers dealing with the Friuli region (e.g. Aoudia et al., 2000; Bajc et al., 2001), a simple 1D model for the region (FRIUL7W) derived

by Fäh et al (1993) and based on travel-time inversion results of Mao and Suhadolc (1992), which we will rename 1D_DST (Figure 2(b)), was used to compute synthetic seismograms. The main differences between the 2D model and 1D_DST are the low-velocity wedge below the pre-Alpine belt (i.e. near Belluno), and the presence of an important low-velocity channel characterizing the 1D model at a depth of about 3-6 km (see Table 1). The reason for these differences is that 1D_DST is an average structure valid for the whole of Friuli, particularly the central area, whereas the proposed 2D model is based on reflection and refraction seismic lines along and around our profile, which cuts the lower Friuli plain. In this work, we try to find "equivalent" 1D models that can reproduce, within a given tolerance and for a given source, the ground motion computed with the complex two-dimensional structure. At the same time, we would like to verify the representativeness of the 1D_DST model with respect to the proposed 2D structure. The parameter selected for this comparison is peak ground velocity (PGV), one of the most useful parameters for engineering seismology (e.g. Bommer and Alarcon, 2006), computed for receivers located at variable distances from the source. As our seismic sources are very simple point sources and we only calculate low frequencies, PGV is the most appropriate strong-motion intensity parameter for this study.

Method

In order to obtain homogeneous results for all computations (1D, 2D and 3D), we adopt a standard fourth-order, staggered-grid finite-differences numerical code (FDM) previously used in Aochi and Madariaga (2003 and references therein) for near-field strong ground motion simulations. We chose this method since it can model waveforms using laterally-heterogeneous, smoothly-varying structures. Anelastic attenuation is included via a damping factor specified for each layer (Graves, 1996). The model area corresponds to the coordinates (X, Y) shown in Figure 1 with dimensions of: 0 to 120 km along the X axis, -80 to 40 km along the Y axis and 0 to 20 km in depth (Z axis). However, all the simulations except for the first examples (Figures 3 and 4) are run in the narrow region (Y=-10 to 10 km), as no lateral heterogeneity is assumed along the Y axis. The efficient,

perfectly matching layer absorbing boundary conditions are adopted (Collino and Tsogka, 2001). For some demonstrative simulations for a preliminary 3D structure model, the area is extended from -40 km to 80 km in the Y axis. A pure strike-slip point-source of magnitude M_w 5 with a bell-shaped source-time function of 1.2 s has been employed for the generation of seismic waves, as tested previously in Douglas et al. (2006). Three earthquake positions are chosen as in Figure 2. Source (I) and (II) are located at the NW corner of the cross-section, (X, Y) = (10 km, 0 km), shown in Figure 1, and Source (III) is assumed to be in the SE corner, (X, Y) = (100 km, 0 km), so as to be roughly consistent with the observed seismicity in the Friuli region. The fault strike is taken to be 60º anticlockwise in the coordinate (X, Y), which is reasonable with respect to the geological situation in this region. This configuration also means that the considered cross-section is not on the nodal plane of wave radiation patterns.

Due to the computational limitations imposed by the grid size of the model and the low shear-wave velocity of the upper layers, the maximum frequency of the computation is set at 0.6 Hz, consistent also with the duration of the given source-time function. Note that our FDM grid spacing does not take into account certain thin layers of low velocity shown in Table 1 since these layers are thinner than the grid resolution and, hence, they are neglected in the numerical modelling. However, this does not lose the characteristcs of the basin and the differences between the considered models. Sophisticated approaches for homogenizing the medium do exist (e.g. Eisner and Clayton, 2002), but we do not aim to carry out complex seismic hazard assessment in this paper. We think that our simplified numerical treatment is sufficient for the following discussion. On the basis of the physical parameters involved, we adopt a space-step of 200 m and a time-step of 0.01 s. In each simulation, all sources and receivers lie along the same line located in the middle (with respect to width) of the models. The synthetic seismograms in three components are stacked at each receiver point and the PGV used in this study is the geometrical mean of amplitudes of horizontal ground velocity (in agreement with current standard practice) following low-pass filtering up to 0.6 Hz.

Equivalent 1D models

Starting from the 2D structure, we produce several 1D structural velocity models, that can be gathered into two groups. The first group contains "average" models obtained by averaging, at each depth level, the model parameters between the source and the receiver positions. This procedure was successfully used by Douglas et al. (2006) to conduct modelling using the structure under the Pyrenees on the French-Spanish border. The second group contains models, which we will refer to as "receiver-based" models, and are obtained by considering the 1D model parameters under each receiver.

Considering, in addition, the important asymmetry of the 2D model in terms of geological structures, and hence of physical parameters, and the possible earthquake-prone areas in the region, we define two sets of seismic sources, one near the left and the other near the right-hand side of the model. The source depth was kept constant, at 7 km, (except for one test using a depth of 15km) the value being chosen on the basis of the average seismic activity depth in the area of interest. In this way, we can analyze the influence of the main heterogeneities in a seismically plausible context. Figures 1 and 2 show the positions of the sources and receivers.

Simulations

First of all, we show some simulations using a 3D model for the region of interest to demonstrate that a 2D model is sufficient for the travel paths considered in this study. There is no 3D model available for the whole of our study area and, therefore, we derive an approximate model by interpolating between our 2D section and the detailed 3D model of Gentile et al. (2000), which covers the area to the north of the travel paths modelled here (see Figure 1). To the SW of our 2D section, no 3D crustal structural models seem to have been published, therefore, since this area is a plain, we assumed that our 2D section could be extended south-westwards parallel to our O-B

section. Michelini et al. (1998) derive a 3D model of Slovenia to the east of our study area, which we originally planned to use to constrain our 3D model, but their model does not have sufficient vertical resolution for our purpose. Based on the geological context, it is reasonable to assume that the northern area in the mountains is a hard rock area, as found in Gentile et al. (2000), while the basin structure extends out to the southern part of the large Friuli plain. We, thus, assume the model of Gentile et al. (2000) to the north of Y = 70 km and the 2D cross-section model to the south of Y = 10 km. We linearly interpolate between both models for Y = 10 to 70 km. Beneath a depth of 10 km, we assume the 1D stratified model shown in the 2D cross-section model for all locations.

Figure 3, shows snapshots of the wave propagation in the constructed 3D and 2D structure models. A comparison of seismograms from 2D and 3D modelling at four locations along the array is shown in Figure 4, after applying a low-pass filter with a cut-off at 0.6 Hz. We observe some differences in seismograms once the waves enter the basin structure. In particular, the reflecting waves due to the basin edge appear in the results using the 3D model (see the snapshot at 40 s). Thus the duration of signals is a function of the horizontal location. Nevertheless, even though there are differences in waveforms, the wave amplitudes at each station are compatible because of the characteristic of the source-station paths. It would be interesting to quantitatively study the effect of a 2D and a 3D structure in this region, but our preliminary 3D model is not yet validated, as it is not known how far north the basin structure continues in the Y direction. Therefore, we do not aim to quantify 3D effects in this article and hence 3D effects are not discussed further.

Results

In this section, we present the simulation results based on the 2D and the various 1D models. Figures 5, 6 and 7 show the seismograms simulated using the 2D model and those for each average 1D model at various distances for Sources (I), (II) and (III), respectively. It should be noted that the seismograms at each distance (every 10 km) are obtained through an individual simulation using the

corresponding “average” 1D model or “receiver-based” 1D model, while the simulations using the 2D model and the 1D-DST model provide with what? the seismograms at any receiver within a single simulation. In other words, results for different receiver positions in “average” and “receiver-based” 1D models show the outcome of various simulations. We show here only the seismograms obtained with “average” 1D models, but any other 1D model shows similar tendencies though /through?? amplitude changes and phase shifts according to the given structure.

Some clear differences are observed in Figures 5, 6 and 7 due to the existence of the basin structure, while there is little difference near the source (e.g. compare X = 20 km in Figures 5 and 6, and X= 90 km in Figure 7) where the travel path from the source to the receiver is quite vertical. The shallow source (I) shows higher amplitudes and complex waveforms due to the 2D geometry between the source and the basin (receiver position at X = 50 km in Figure 5). This effect becomes less clear at greater distances (X = 80 km). This implies that the amplification at X = 50 km originates, particularly, from the geometry of the basin edge and the incident waves and it is confirmed that a suitable 1D model could exist for a sufficiently large basin. We also noticed that the results from the average 1D model overestimate the amplitude for locations outside the basin (e.g. X = 110 km), because the shallow structure has a very low velocity due to the averaging compared to the original 2D model. Comparing the results for the 2D and 3D models, the seismograms in any 1D structure are expected to be very simple such that the direct waves are dominant, because there is no lateral heterogeneity (see Figures 5 to 7). However, the overestimation of PGV changes according to the chosen 1D model.

The 2D effect is localized in the basin when the hypocentral depth is larger (Source (II) in Figure 6). This is because the incident waves become more vertical. On the other hand, we do not observe the same 2D effect for Source (III) in Figure 7. This implies that the average 1D structure is sufficient because the change in lateral heterogeneity to the SE is very smooth compared to the

other side. This indicates the importance of the basin-edge structure. In addition, the average model does not work for close distances (e.g. X = 10 km) for the same reasons as for source (I) in Figure 5.

Hereafter, the results are presented in terms of PGV versus epicentral distance instead of versus model-related distance. We start with the results relative to Source (I). Figure 8 shows the PGVs computed up to an epicentral distance of 100 km (i.e. up to X = 110 km in terms of receiver position), which are the most interesting. An important amplification due to the 2D basin structure is clearly seen at 20 – 40 km distances, as observed in the waveforms (at X = 50 km) in Figure 5, while all 1D structure models show simple decay of PGV with distance. This is due to the geometrical effect of the basin edge (wave focusing). The absolute differences between the PGVs obtained using the 2D and each 1D model are also shown to quantitatively investigate the range of distances where the fit between the two models show good agreement. Both 1D structures give similar results to the 2D case for locations outside the basin.

Since we also want to understand the role played by the low-velocity wedge as a function of the propagation path, we next compare the simulations for source (II) in Figure 9. As expected from the seismograms (Figure 6), the 2D effect is less clear for this scenario compared to source (I). We confirm that PGVs using the "receiver-based" 1D models fit the results from 2D simulations better than those obtained from using the "average" 1D models. Finally, Figure 10 compares the results for source (III) corresponding to the seismograms shown in Figure 7. We find that the results using "average" and "receiver-based" 1D models provide quite a good agreement with those from 2D simulations.

If we look at the performance of the 1D_DST model, we can notice from Figures 6 and 7 that it reproduces the 2D PGV values in the whole considered distance range quite well, especially for

epicentral distances greater than 30 km, where it gives the best results. At smaller epicentral distances it is, however, still one of the best models. The only time when the 1D_DST model gives the worst performance is for source (III) (Figure 8). This is particularly evident when we compare its performance with respect to the 1D models obtained by the averaging process, and for small epicentral distances. The better performance of the 1D_DST model for source (I) is probably because the 1D_DST model has a low-velocity layer in the depth range 3.5-6 km, whose effect is partly balanced by the low-velocity wedge in the 2D model that roughly spans the depth range 2.5 to 4 km.

Conclusions

We have performed a series of simulations of seismic wave propagation from potential earthquakes to evaluate how the 2D (in the NW-SE direction) geological structure of the Friuli basin affects ground motions, particularly in terms of peak ground velocity (PGV). The decay of PGV with source-receiver distance from the 2D modelling is compared to that obtained from 1D modelling, using a standard model for seismological studies in this region, one obtained by averaging the 2D model along the source-receiver distance and one based on the local structure under the receiver. Synthetic seismograms are computed using a finite-difference technique for point sources with an upper frequency cut-off of 0.6 Hz. 2D effects are clearly seen, particularly in the centre of the sedimentary basin, for certain earthquake scenarios. The analysis of the role played by the main heterogeneities on the propagating wavefield permits us to conclude that an acceptable fit to the 2D PGV values for the entire section is possible using a series of 1D models for the Friuli region except

for shallow earthquakes located to the north-west of the basin where the structure of the basin edge is complex.

Although we concentrate on PGV in this article, our simulations are also interesting with respect to the simulated waveforms (Figures. 5, 6 and 7). It is the complete time-history of shaking that is ultimately responsible for damage during earthquakes not simply peak ground parameters, such as PGV. The PGV is due, in most cases, to the direct shear wave except for the basin area in the 2D model, where the locally amplified wave in the low-velocity zone follows after the direct waves and propagates as a surface wave. More complex waveforms, with longer durations, are seen in the 3D simulations, compared with the 2D simulations, with late wave arrivals coming from reflections off the northern basin edge, although these waves do not generally contribute the largest amplitudes in the earthquake shaking. Simpler, generally shorter duration waveforms are seen in the simulations using 1D structural models due to the lack of reflected waves off the basin edges and a lack of surface waves generated at the basin edges. It seems that the wave, amplified by the basin, is large for an earthquake at the western side of the basin, probably because of the end shape of the basin with respect the earthquake location. It should be noted that whether the basin effect is 1D, 2D or 3D depends on the location of the earthquake, even for the same basin. Once generated, the surface wave continues to propagate further outside the basin (e.g. see Figure 5). Its amplitude is smaller than the direct wave, so that the difference in PGV is not so important in this study. However, it is clear that the seismic wave energy is transferred very late in the 2D model. The insights obtained in 1D/2D models could be useful for rapid analyses of the earthquake source and seismic hazard. Nevertheless, we have to keep in mind that examining only PGV does not tell the whole story because the general purpose of synthesizing ground motion is not to simply replicate empirical ground-motion prediction equations for strong-motion intensity parameters (e.g. PGV), but generally to synthesize complete waveforms of possible strong ground motion. Full analysis for a more realistic 3D geological structure for this region should be a future goal.

Acknowledgments

This study was financially supported by the contract "Contratto tra Dipartimento di Scienze della Terra e Regione Autonoma FVG, Direzione Regionale della Protezione Civile per la gestione della Rete Accelerometrica del Friuli Venezia Giulia (Contratto 6/06, Delibera Giunta Regionale 3425, dd 29/12/05)". A part of the numerical modelling was also carried out within the BRGM research program on seismic risk in 2007 and 2009. We thank G. F. Gentile and G. Bressan for providing the files for the 3D crustal model of Gentile et al. (2000). Finally, we thank associate editor Dr L. Hutchings and two anonymous reviewers for their constructive and detailed comments on a previous version of this article.

[6]References

Aochi, H. and Madariaga R., 2003, The 1999 Izmit, Turkey, earthquake: Non-planar fault structure, dynamic rupture process and strong ground motion, *Bull. Seism. Soc. Am.*, 93, 1249-1266.

Aoudia, A., Sarao', A., Bukchin, B. and Suhadolc, P., 2000. The Friuli 1976 event: a reappraisal 23 years later. *Geophys. Res. Lett.*, 27(4), 573-576.

Bajc, J., Aoudia, A., Sarao', A., and Suhadolc, P., 2001. The 1998 Bovec-Krn mountain (Slovenia) earthquake sequence. *Geophys. Res. Lett.*, 28(9), 1839-1842.

Bommer, J. J., and Alarcon, J. E. 2006. The prediction and use of peak ground velocity. Journal of Earthquake Engineering, 10(1), 1–31.

Collino, F. and Tsogka, C., 2001. Application of the perfectly matched absorbing layer model to the linear elastodynamic problem in anisotropic heterogeneous media, *Geophysics*, 66, 294-307.

Douglas, J., Aochi, H., Suhadolc, P. and Costa, G., 2007, The importance of crustal structure in explaining the observed uncertainties in ground motion estimation, *Bull. Earthq. Engineering,* 5, 17-26.

Douglas, J., Aochi, H., Suhadolc, P. and Costa, G., 2006. On the applicability of one-dimensional crustal structures for ground-motion simulation. Proc. First European Conference on Earthquake Engineering and Seismology, Geneva, Switzerland, 3-8 September 2006, Paper number 18 (CD-ROM).

Eisner, L. and R. W. Clayton, 2002, Equivalent medium parameters for numerical modeling in media with near-surface low velocities, *Bull. Seism. Soc. Am.*, 92, 711-722.

Fäh, D., Suhadolc, P. and Panza, G. F., 1993. Variability of seismic ground motion in complex media: the case of a sedimentary basin in the Friuli (Italy) area. In: R. Cassinis, K. Helbig and G.F. Panza (Eds.), Geophysical Exploration in Areas of Complex Geology, II. *J. Appl Geophys.*, 30, 131-148.

Gentile, G.F., Bressan, G., Burlini, L., De Franco, R., 2000. Three-dimensional Vp and Vp/Vs models of the upper crust in the Friuli area (Northeastern Italy). *Geophys. J., Int.*, 141, 457-478.

Graves, R. W., 1996, Simulting seismic wave propagation in 3D elastic media using staggered-grid finite differences, *Bull. Seism. Soc. Am.*, 86, 1091-1106.

Graves, R. W. and D. J. Wald, 2001, 3D seismic resolution analysis of finite fault source inversion using 1D and 3D Green's functions, Part I: Strong Motions, *J. Geophys. Res.*, 106, 8745-8766.

Liu, P. and R. J. Archuleta, 2004, A new nonlinear finite fault inversion with three-dimensional Green's functions: Application to the 1989 Loma Prieta, California, earthquake, *J. Geophys. Res.*, 109, B02318, doi:10.1029/2003JB002625.

Liu, P., S. Custodio and R. J. Archuleta, 2006, Kinematic inversion of the 2004 M6.0 Parkfield earthquake including an approximation to site effects, *Bull. Seism. Soc. Am.*, 96, S143-S158.

Mao, W.J. and Suhadolc, P., 1992. Simultaneous inversion of velocity structures and hypocentral locations: application to the Friuli seismic area NE Italy. *Pure and Applied Geophys*., 138, 267-285.

Michelini, A., Živčić, M. and Suhadolc, P., 1998. Simultaneous inversion for velocity structure and hypocenters in Slovenia. *J. Seism.*, 2, 257-265.

Wald, D. J. And R. W. Graves, 2001, Resolution analysis of finite fault source inversion using 1D and 3D Green's functions, Part II: Combining Seismic and Geodetic Data, *J. Geophys. Res.*, 106, 8767-8788.

Wu, C., M. Takeo and S. Ide, 2001, Source process of the Chi-chi earthquake: A joint inversion of strong motion data and global positioning system data with a multifault model, *Bull. Seism. Soc. Am.*, 91, 1128-1143.

Tables

Depth (km)	V_p (m/s)	V_s (m/s)	ρ (kg/m^3)	Quality factor
0	1040	600	2000	20
0.4	3460	2000	2300	60
3.2	5200	3000	2600	100
6	5630	3250	2600	100
9	6410	3700	2700	400
12	6670	3850	2800	400

Depth (km)	V_p (m/s)	V_s (m/s)	ρ (kg/m^3)	Quality factor
0	1500	600	2000	24
0.04	3500	1800	2300	108
0.10	4500	2500	2400	500
0.30	5550	3050	2400	1219
1	5880	3240	2600	1295
3.25	5570	3030	2600	606
4.5	5550	3020	2600	602
5	5570	3030	2600	606
6.25	5880	3250	2600	1300
10.9	6450	3750	2600	3003
11.75	6470	3770	2600	3012
14.25	6500	3800	2600	3039
19.25	6550	3820	2600	3058

Table 1 – Left: physical parameters of the 2D model layers under the receiver at 40 km. Right: physical parameters of the 1D_DST model layers (standard model for seismological applications in the Friuli region). Note that each model features a thin low-velocity sedimentary layer at the surface. Depth refers to the top of each layer.

Figure Captions

Figure 1 – Map of the studied area in this paper. 2D cross-section given in Figure 2 corresponds to the line OB. The supposed earthquake source at (X, Y) = (10 km, 0 km) and the station locations are shown as a focal mechanism and triangles in blue. For further discussion, a preliminary 3D geological model is constructed in the black box area (120 km × 120 km), compiling the cross-section OB and the tomographic result by Gentile et al. (2000) (yellow box)..

Figure 2 – (a) the proposed 2D model with the locations of some major towns in the area (cross-section OB in Figure 1.). (b) the 1D_DST model for the NE Italian area (see text). In both cases the S-wave speed is shown. The simulated source locations are shown: (I) (X, Y) = (10 km, 0 km) with a depth of 7 km, (II) the same epicenter as (I) but with a depth of 15 km, and (III) (X, Y) = (100 km, 0 km) with a depth of 15 km, represented by stars. The receivers are located every 5 km on the ground surface along the cross-section OB.

Figure 3 – Snapshots of the simulated wave propagation in the 3D and 2D structures. Each component of horizontal ground velocity is shown. The source (I) is presented by a focal mechanism (depth = 7 km) and the stations are indicated by stars.

Figure 4 – Comparison of seismograms simulated in the 3D (dotted) and 2D (solid) structure models (see also Figure 3) along the station array at distances of X = 25km, 55 km, 85km and 115 km from top to bottom. The left and right columns are the X and Y components of the ground velocity low-pass filtered up to 0.6 Hz.

Figure 5 – Comparison of seismograms simulated in the 2D structure model with respect to each average 1D model at the shown distance. Source position is (I). See also the caption of Figure 4.

Figure 6 – Comparison of seismograms simulated in the 2D structure model with respect to each average 1D model at the shown distance. Source position is (II). See also the caption of Figure 4.

Figure 7 – Comparison of seismograms simulated in the 2D structure model with respect to each average 1D model at the shown distance. Source position is (III). See also the caption of Figure 4.

Figure 8 – (top) PGV values simulated in the various structure models against receiver positions along cross-section OB for source model (I), (X, Y) = (10 km, 0 km) at 7 km depth. (bottom) Ratios of PGVs obtained using the 2D and the 1D models.

Figure 9 – (top) PGV values against simulated in the various structure models vs. receiver positions along cross-section OB for source model (II), (X, Y) = (10 km, 0 km) at 15 km depth. (bottom) Ratios of PGVs obtained using the 2D and the 1D models.

Figure 10 – (top) PGV values against simulated in the various structure models vs. receiver positions along cross-section OB for source model (III), (X, Y) = (100 km, 0 km) at 7 km depth. (bottom) Ratios of PGVs obtained using the 2D and the 1D models.

Figures

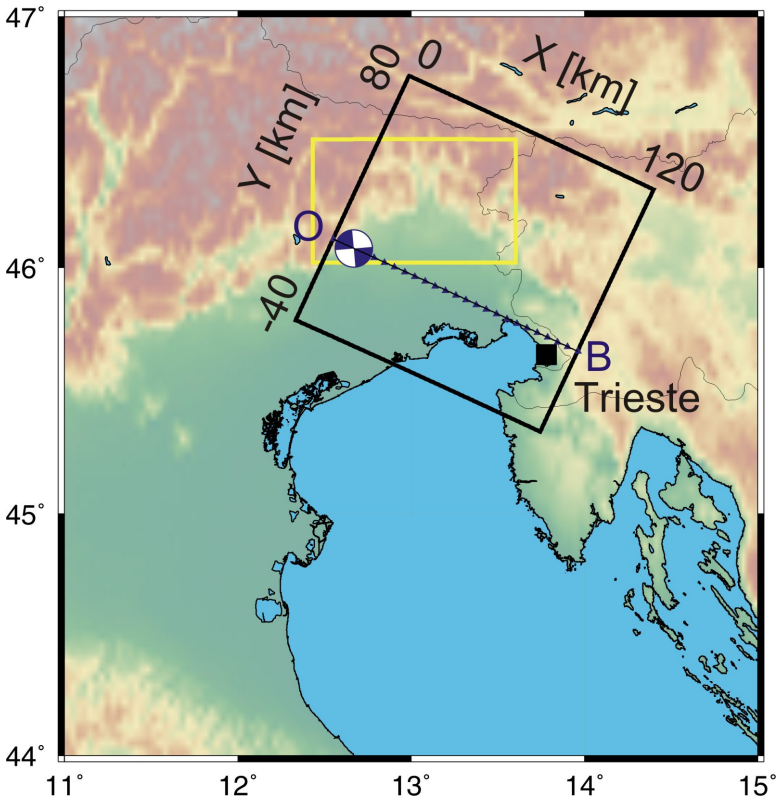

Figure 1:

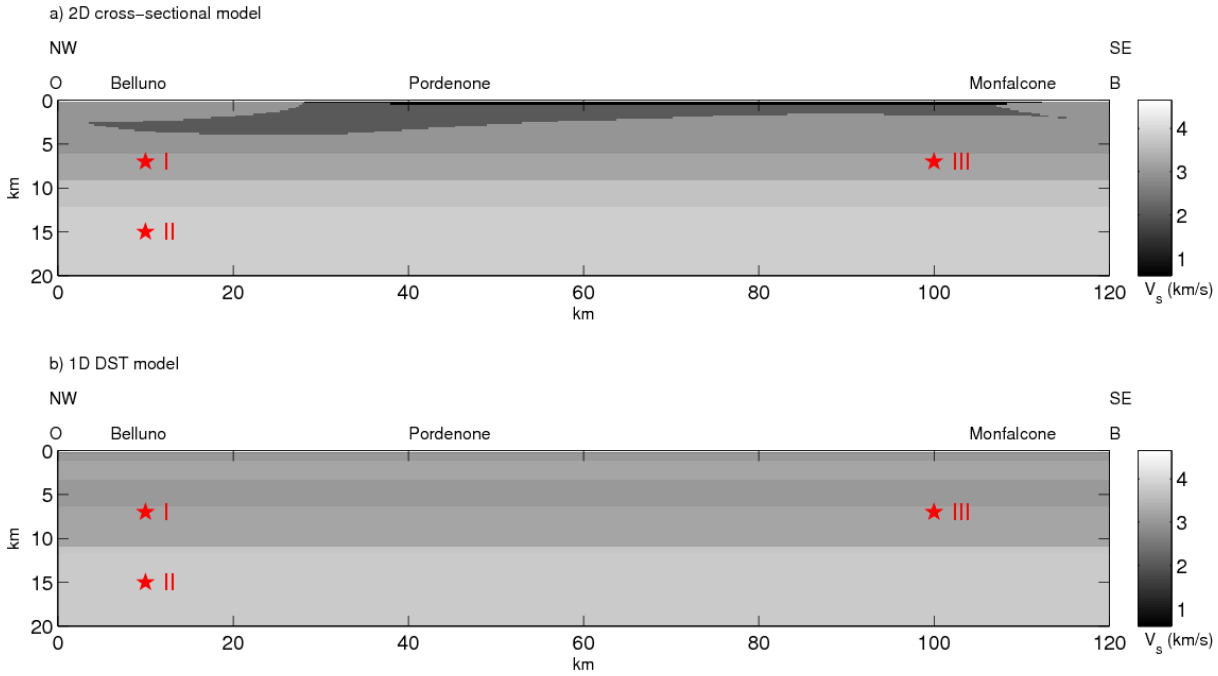
a) 2D cross–sectional model
NW
SE
O
Belluno
Pordenone
Monfalcone
B
0
5
10
15
20
km
I
II
III
0
20
40
60
80
100
120
km
4
3
2
1
V_s (km/s)
b) 1D DST model
NW
SE
O
Belluno
Pordenone
Monfalcone
B
0
5
10
15
20
km
I
II
III
0
20
40
60
80
100
120
km
4
3
2
1
V_s (km/s)

Figure 2

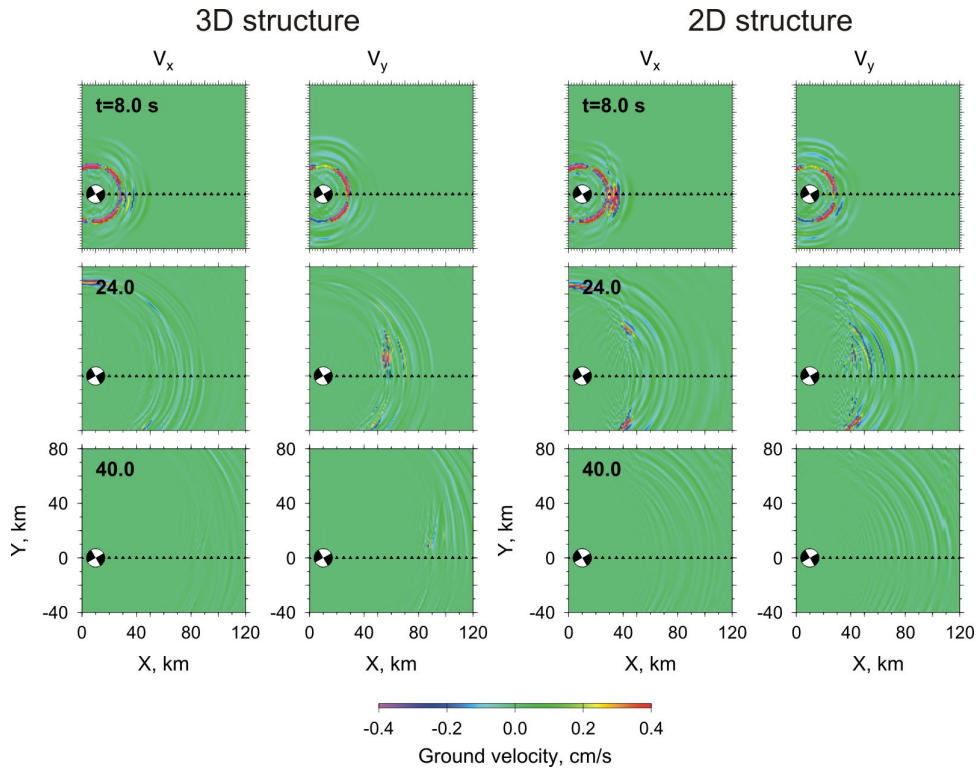
3D structure
2D structure
Vx
Vy
Vx
Vy
t=8.0 s
t=8.0 s
24.0
24.0
40.0
40.0
80
40
0
-40
Y, km
0
40
80
120
X, km
-0.4
-0.2
0.0
0.2
0.4
Ground velocity, cm/s

Figure 3.

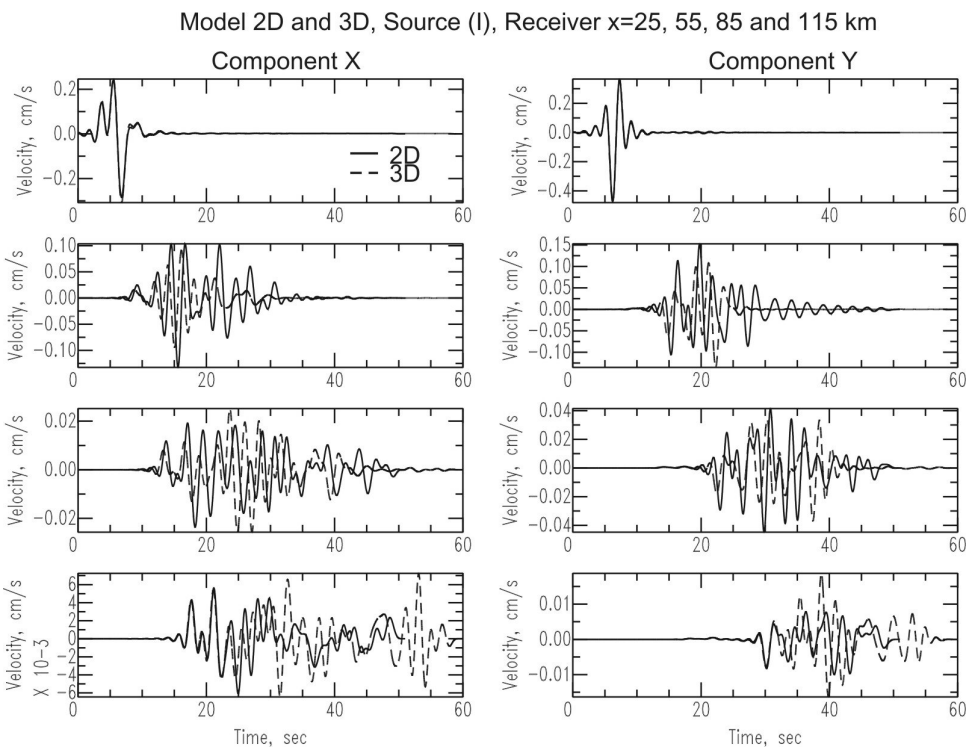
Model 2D and 3D, Source (I), Receiver x=25, 55, 85 and 115 km
Component X
Component Y
2D
3D
Velocity, cm/s
Velocity, cm/s X 10−3
Time, sec

Figure 4.

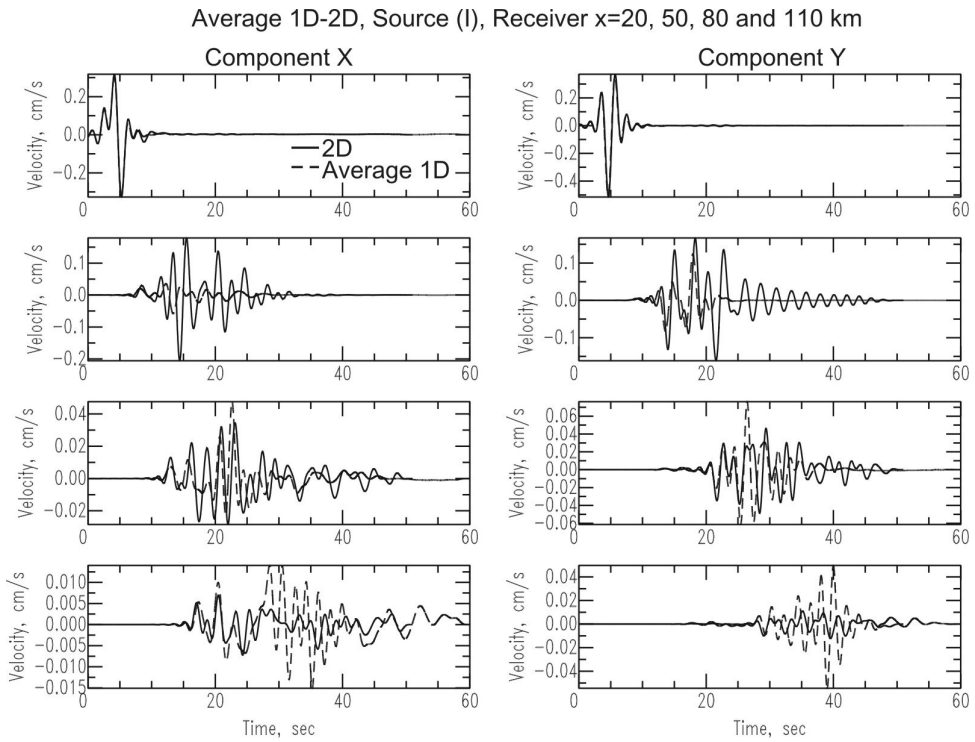
Average 1D-2D, Source (I), Receiver x=20, 50, 80 and 110 km
Component X
Component Y
2D
Average 1D
Velocity, cm/s
Time, sec

Figure 5

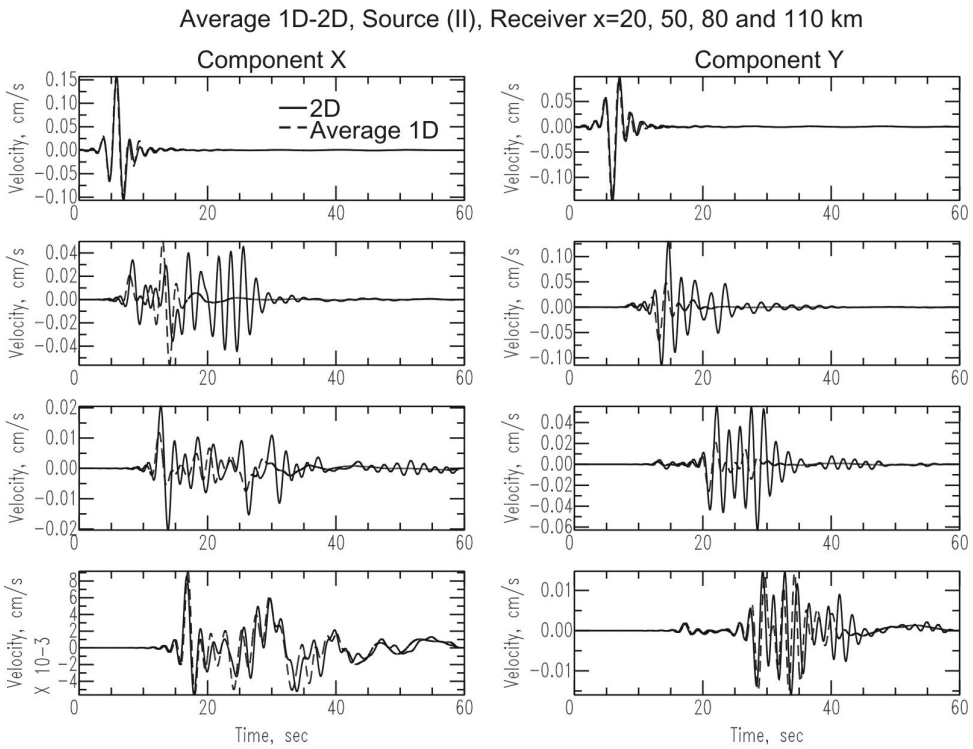
Average 1D-2D, Source (II), Receiver x=20, 50, 80 and 110 km
Component X
Component Y
2D
Average 1D
Velocity, cm/s
X 10−3
Time, sec

Figure 6.

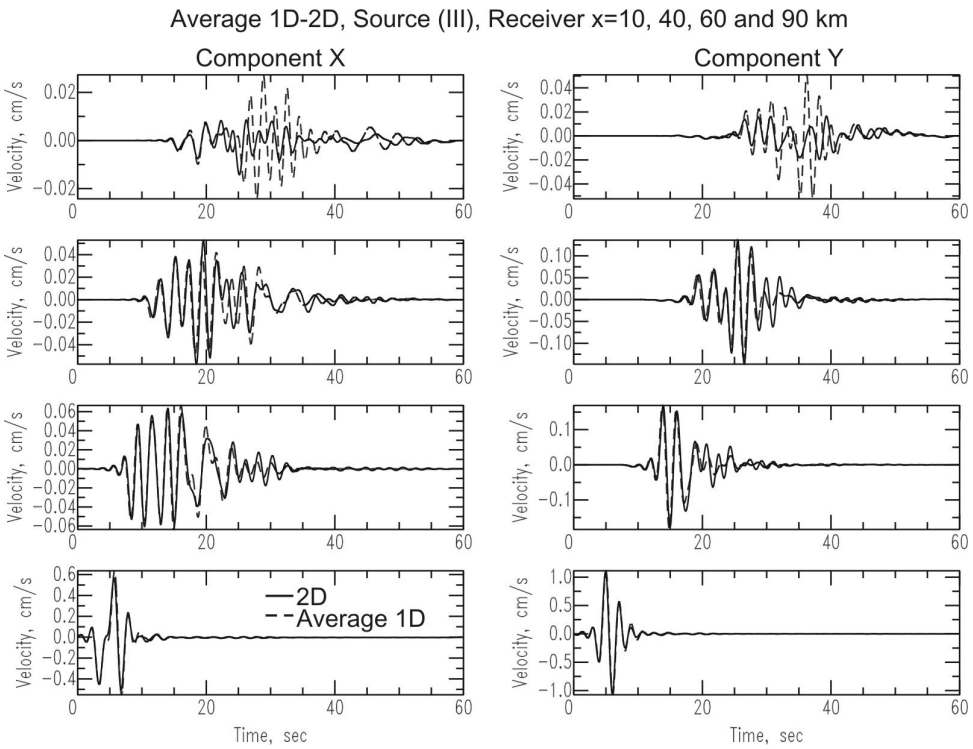
Average 1D-2D, Source (III), Receiver x=10, 40, 60 and 90 km
Component X
Component Y
Velocity, cm/s
2D
Average 1D
Time, sec

Figure 7.

Source (I)

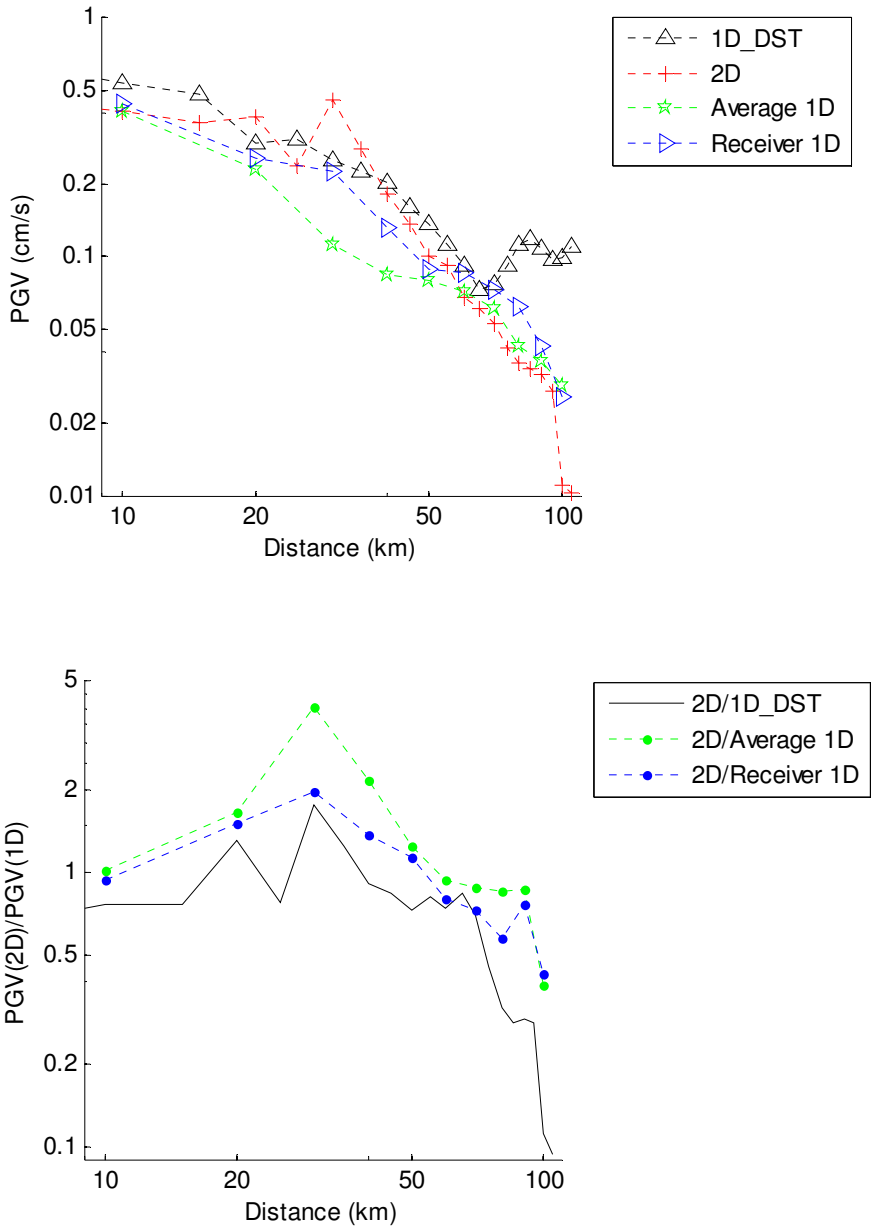

Figure 8

1 Source (II)

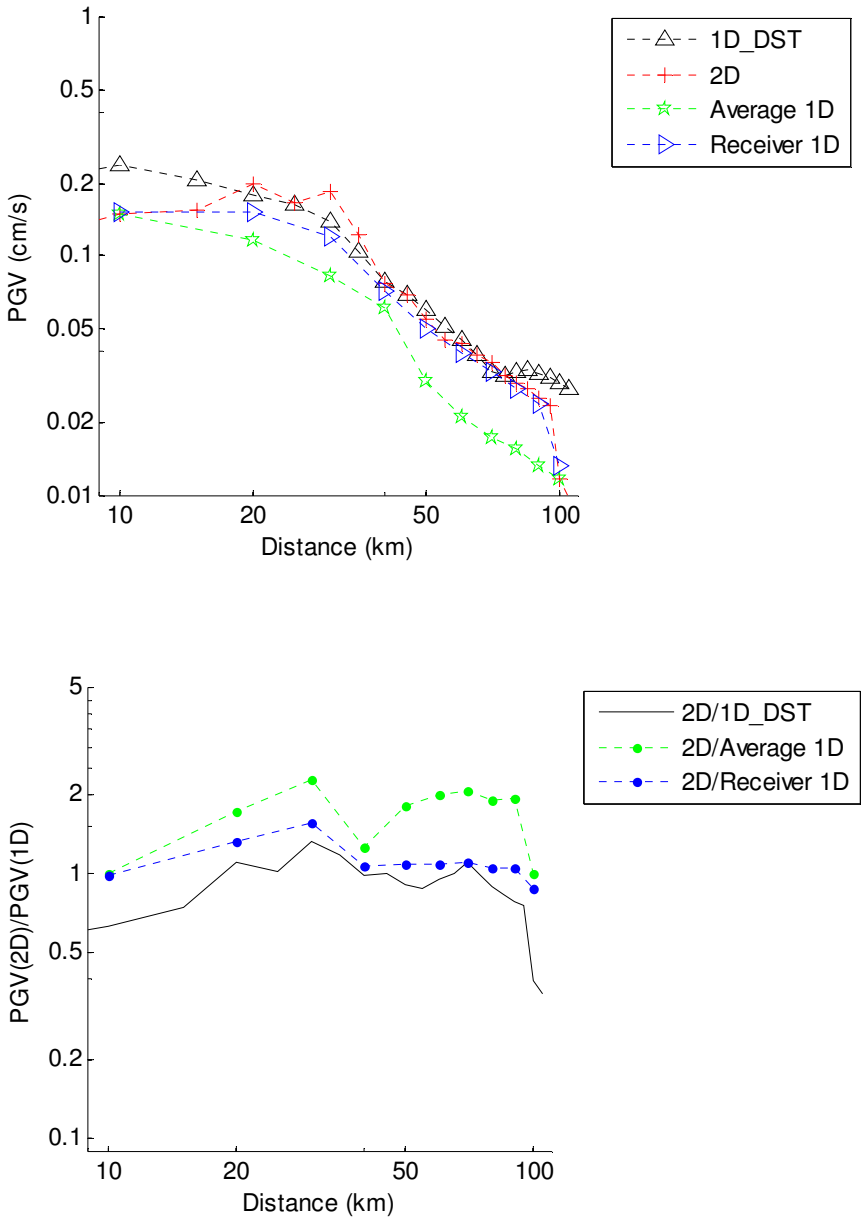

2
3
4 Figure 9
5
6

Source (III)

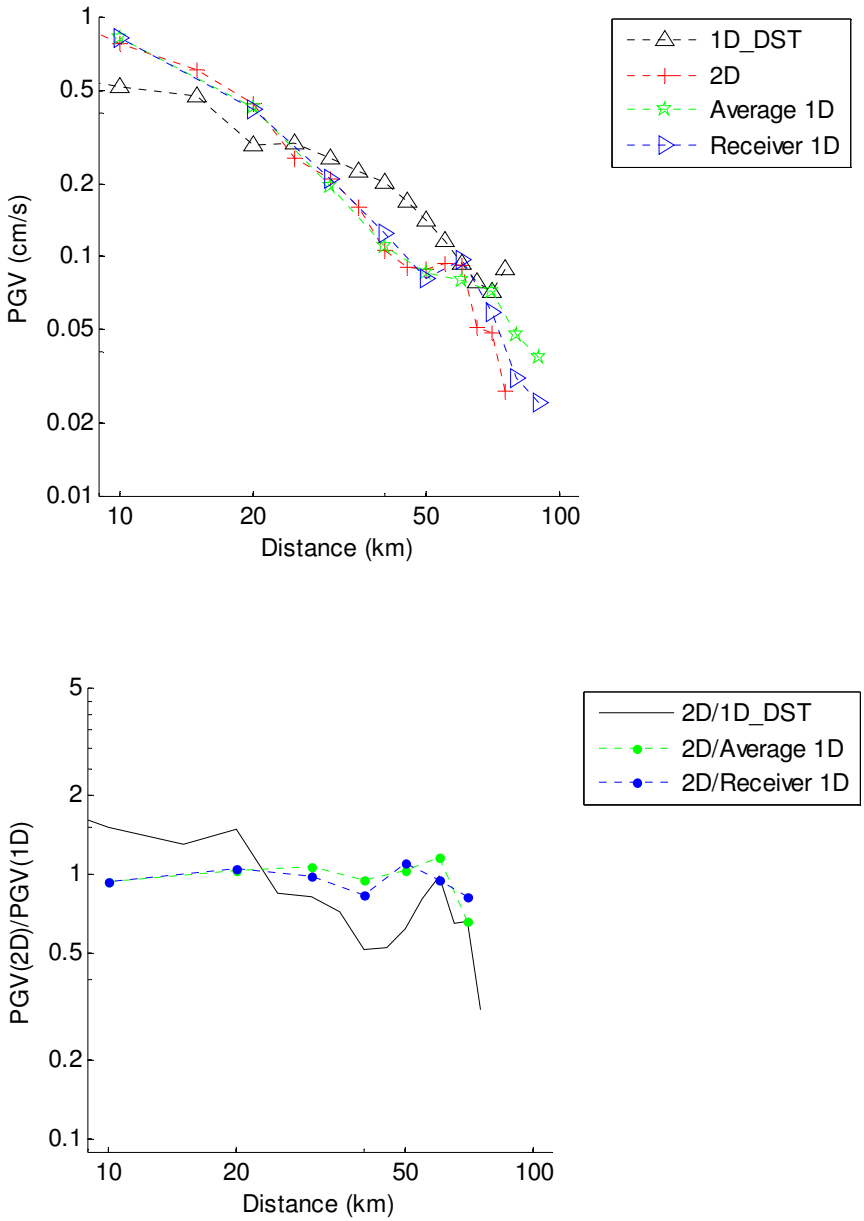

Figure 10